

# Repeated Pleistocene glaciation of the East Siberian continental margin

Frank Niessen<sup>1\*</sup>, Jong Kuk Hong<sup>2\*</sup>, Anne Hegewald<sup>1</sup>, Jens Matthiessen<sup>1</sup>, Rüdiger Stein<sup>1</sup>,  
Hyoungjun Kim<sup>2</sup>, Sookwan Kim<sup>2,3</sup>, Laura Jensen<sup>1</sup>, Wilfried Jokat<sup>1</sup>, Seung-Il Nam<sup>2</sup> and Sung-Ho Kang<sup>2</sup>

**During the Pleistocene glaciations, Arctic ice sheets on western Eurasia, Greenland and North America terminated at their continental margins<sup>1-4</sup>. In contrast, the exposed continental shelves in the Beringian region of Siberia are thought to have been covered by a tundra landscape<sup>5-7</sup>. Evidence of grounded ice on seafloor ridges and plateaux off the coast of the Beringian margin, at depths of up to 1,000 m, have generally been attributed to ice shelves or giant icebergs that spread oceanwards during glacial maxima<sup>8-12</sup>. Here we identify marine glaciogenic landforms visible in seismic profiles and detailed bathymetric maps along the East Siberian continental margin. We interpret these features, which occur in present water depths of up to 1,200 m, as traces from grounding events of ice sheets and ice shelves. We conclude that the Siberian Shelf edge and parts of the Arctic Ocean were covered by ice sheets of about 1 km in thickness during several Pleistocene glaciations before the most recent glacial period, which must have had a significant influence on albedo and oceanic and atmospheric circulation.**

For the Last Glacial Maximum (LGM), about 20,000 years (20 kyr) ago, most of the present Chukchi and East Siberian seas (Fig. 1) are thought to have been free of ice sheets<sup>1,2,5-7,13,14</sup> ([http://instaar.colorado.edu/QGISL/ak\\_paleoglacier\\_atlas/gallery/index.html](http://instaar.colorado.edu/QGISL/ak_paleoglacier_atlas/gallery/index.html)). Invasion of atmospheric moisture from a predominantly Atlantic source region was lowered by the barrier of the Eurasian Ice Sheet<sup>2,13</sup> combined with a reduced and more southerly meridional overturning circulation in the North Atlantic<sup>15</sup>. With the sea level 120 m lower than at present<sup>16</sup> a land bridge existed between the Asian and American continents<sup>5-7</sup>. Evidence for LGM ice is local and minimal in extent as it is also elsewhere in East Siberia in contrast to earlier glaciations<sup>5-7,13,14</sup> (Fig. 1a). However, studies of the Chukchi Borderland suggest ice grounding attributed to ice shelves extending from the northern margin of the Laurentide Ice Sheet combined with an ice rise formed over the borderland<sup>10,11</sup>. A chronology is proposed that this may have last occurred during the LGM (ref. 9) and at least during two earlier and larger glaciations tentatively dated as middle and late Pleistocene with ice grounding as deep as 900 m below present sea level (m.b.p.s.l.; refs 9-11). Within the timeframe of these earlier glaciations, erosion by grounded ice has been recorded as far as the Mendeleev Ridge at 850 m.b.p.s.l. (ref. 17), for which the proposed source region is on the Chukchi Borderland or the East Siberian Shelf<sup>11,17</sup>.

Here the questions arise: did ice sheets exist on the East Siberian Shelf during earlier Pleistocene glaciations? Is the lack of ice cover during the LGM a unique minimum? To address this problem we

present acoustic data from the East Siberian continental margin (ESCM) obtained during two Arctic Ocean expeditions (Fig. 1c). It is well established that evidence of ancient ice sheets is provided by the presence of glaciogenic landforms preserved in the geological record along submarine continental margins<sup>10,18-20</sup>. These are best documented in data obtained by swath sonar, sediment echosounding and seismic reflection methods. These tools can be used to investigate former subglacial morphology, characterize depositional environments and visualize masses of glacial debris<sup>19</sup>.

On the ESCM we have discovered several sets of streamlined glacial lineations (SGL) between 900 and 1,200 m.b.p.s.l., which are indicative of former ice grounding. They cluster in southwest-northeast directions orthogonal to the ESCM (Figs 2a, 3a). SGL are interpreted as flutes at the base of ice sheets and ice streams<sup>8,10,18</sup>. On top of and adjacent to the Arlis Plateau (Figs 1, 2), four sets of SGL can be distinguished. Ice that formed the youngest and older sets grounded in depths of up to 950 and 1,200 m.b.p.s.l., respectively (Fig. 2a). Likewise, farther west at the ESCM additional sets of SGL are indicated in bathymetric data (Fig. 3a) resembling water depth and orientation of those at the Arlis Plateau. The geometry and pattern are similar to streamlined linear bed forms described from other polar regions and former glaciated continental margins<sup>10,11,18-20</sup>. On the ESCM and the Arlis Plateau, the nearly unidirectional orientation of the bed forms over long distances in combination with the large grounding depths suggest that they were formed by large and coherent ice masses.

On the Arlis Plateau the detailed bathymetry of the youngest SGL provides evidence of both an ice-grounding line on its northern tip and an increase in ice thickness in a southerly direction (Fig. 2a). This indicates that the source area must have been located on the ESCM with northeast- to north-northeast-directed ice flows into the deep ocean (Fig. 1a). This is consistent with seismic evidence for glacial erosion of older strata along the edge of the Chukchi and East Siberian seas<sup>21</sup>. Our interpretation suggests that this erosion was associated with a drastic change in the depositional environment (Figs 2c, 3c, 4c). At some time in the past the sedimentation of progradational, well-stratified sequences ceased, and the deposition of glaciogenic fans in places more than 400 m thick (Fig. 4c) began to dominate the sedimentary accumulation on the ESCM.

These fans consist of glaciogenic wedges and layers intercalated with, and overlain by, hemipelagic sediments (Figs 3b, 4b). The glaciogenic facies can be identified by their structureless transparent character in high-resolution seismic images (Figs 2b, 3b, 4b), which is typical for subglacial and ice-proximal deposits in the Arctic Ocean and along other modern and ancient glaciated marine

<sup>1</sup>Alfred Wegener Institute, Helmholtz Centre for Polar and Marine Research (AWI), Am Alten Hafen 26, 27568 Bremerhaven, Germany, <sup>2</sup>Korea Polar Research Institute (KOPRI), 26 Songdomirae-ro, Yeonsoo-gu, Incheon 406-840, Republic of Korea, <sup>3</sup>University of Science and Technology, 217 Gajung-ro, Yuseong-gu, Daejeon, Republic of Korea. \*e-mail: frank.niessen@awi.de; jkhong@kopri.re.kr

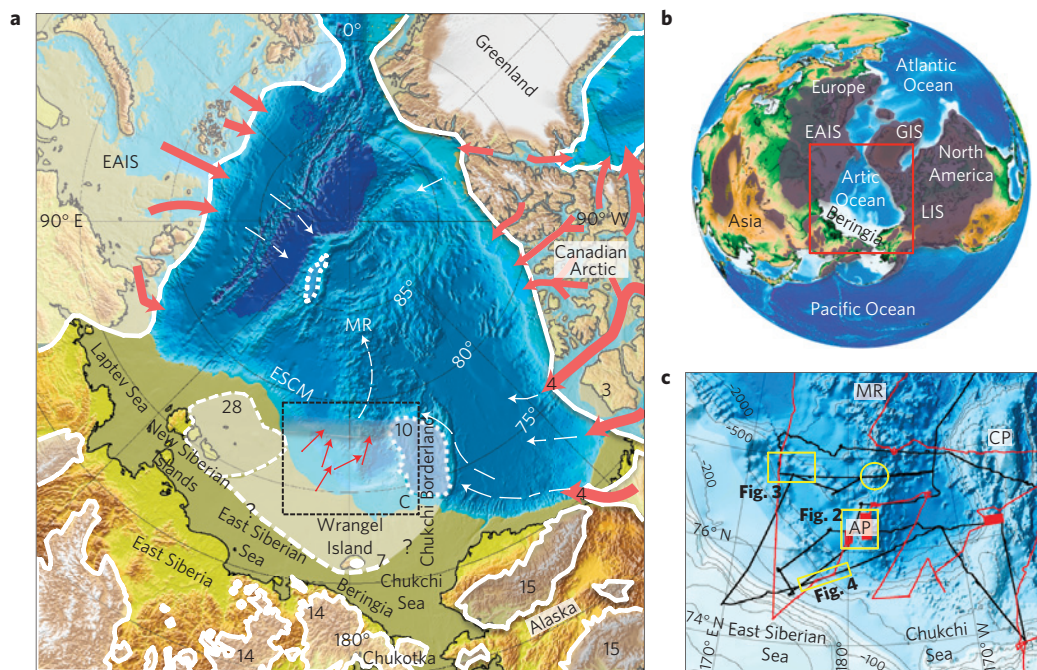


**Figure 1 | Proposed maximum extent of an ice sheet on the East Siberian continental margin (ESCM), Pleistocene ice sheets in the Arctic and area of investigation.** **a**, Maximum Pleistocene glaciations in the Arctic (as far as known, regardless of age). EAIS, Eurasian Ice Sheet; MR, Mendeleev Ridge. Ice boundaries are from ref. 1 unless otherwise marked by number of reference in the map. Maximum glaciation is proposed to have occurred in the middle Pleistocene<sup>11</sup>. LGM ice in Siberia and Alaska is within ice boundaries shown but significantly smaller<sup>14</sup> ([http://instaar.colorado.edu/QGISL/ak\\_paleoglacier\\_atlas/gallery/index.html](http://instaar.colorado.edu/QGISL/ak_paleoglacier_atlas/gallery/index.html)). Red arrows indicate ice-flow directions (Figs 2,3 and 4). White arrows indicate propagation of proposed ice shelves<sup>9,10</sup>. Areas surrounded by white dashed lines are proposed marine ice sheets. Black dashed rectangle marks the location of the map shown in **c**.

**b**, Maximum Pleistocene glaciation in the Arctic according to ref. 1. GIS, Greenland Ice Sheet; LIS, Laurentide Ice Sheet. Red square marks boundary of map shown in **a**. **c**, Bathymetry of the East Siberian–Chukchi continental margin and track lines of expeditions ARK-XXIII/3 (RV *Polarstern*, black) and ARA03B (RV *Araon*, red). AP, Arlis Plateau; CP, Chukchi Plateau. Yellow rectangles mark areas shown in Figs 2–4. Yellow circle marks seamount of the Mendeleev Ridge with evidence of grounded ice<sup>17</sup>.

continental margins<sup>8–10,18–20</sup>. We identified three different types of acoustically transparent facies.

Type 1 is associated with SGL, which form undulated surface areas streamlined parallel to the flow direction of the ice (Figs 2, 3). These are interpreted as subglacial diamicton formed from soft sedimentary deformations at the base of moving ice sheets or ice streams<sup>18,20,22</sup>. In our data SGL are not fully obscured even when covered by up to 20 m of hemipelagic sediments (Figs 2b, 3a,b).

Type 2 is represented by asymmetric wedges of diamicton, recorded between 640 and 680 m.b.p.s.l., of which the surface is undulated with transverse-to-ice-flow ridges (Fig. 4a). In submerged glaciated areas such ridges are often interpreted to have been formed by ice push and/or delivery of deforming bed diamicton at the grounding line<sup>18,23</sup>. The orientation of the ridges is nearly parallel to the shelf edge and the inferred direction of ice flow is northeast, similar to that indicated by SGL. We interpret the ridges as recessional moraines of an ice advance onto hemipelagic sediments (Fig. 4a,b).

Type 3 is characterized by thick sediment wedges or lenses that have smooth surfaces (Figs 3b, 4b). These are interpreted to have been formed by down-slope debris flow of till in grounding-line-proximal areas. These deposits are similar to transparent redeposited facies originating from glacial erosion in troughs and on truncated plateaux and ridges in the Arctic Ocean<sup>8–10,18</sup>.

The intercalation of these three types of glaciogenic deposit with hemipelagic sediments (Figs 3b, 4b) is indicative of episodic input of glaciogenic sediments interrupted by periods without ice sheets on the ESCM and much lower sedimentation rates. We suggest that large quantities of glacially derived debris visible in seismic

data (Figs 3c, 4c) can be explained only by erosion and transport underneath several generations of Pleistocene ice sheets on the ESCM moving north into the Arctic Ocean.

Pleistocene grounding of ice along the ESCM at a depth of 1,200 m.b.p.s.l. implies that ice sheets were thicker than 1 km. Grounding occurs when the height of the ice is equal to the sea level multiplied by the ratio of seawater density over ice density<sup>24</sup>. Assuming a minimal sea level during glacial times of 120 m.b.p.s.l. (ref. 16), ice thickness was more than 1,200 m at the deepest grounding location. A tectonic control on relative sea-level changes can be neglected on the ESCM since the Miocene<sup>21</sup> (Figs 3c, 4c). Simple ice modelling suggests maximum ice thickness for the ESCM of 1 km with slightly more than 2 km on the shelf<sup>25,26</sup>. Numerous publications have disputed this for the LGM (refs 1,2,6,7,13,14) but the modelled ice geometry near the shelf edge could explain our field observations. For ice masses of more than 1 km in thickness along the ESCM we suggest connections to proposed local ice sheets in Beringia (Fig. 1a) forming coherent ice domes at times of maximum glaciation: on the New Siberian Islands there is evidence of middle Pleistocene glaciations pointing to a source region in the outer East Siberian Sea<sup>27</sup>. Erratics found on Wrangel Island are indicative of a larger glaciation before the late Pleistocene<sup>7</sup>. Orientations of glaciogenic bedforms on the Chukchi Borderland that were attributed to formation of an ice rise or marine-based ice sheet<sup>8</sup> are similar to our findings.

As suggested for the Laurentide and Eurasian ice sheets<sup>8,10–12</sup>, our data also imply that ice shelves extended from the ESCM into the Arctic Ocean (Fig. 1a). The grounding line on the Arlis Plateau appears as a ‘lift-off’ zone of a thick ice shelf (Fig. 2a) and not as an active ice margin forming moraines, as described above for the

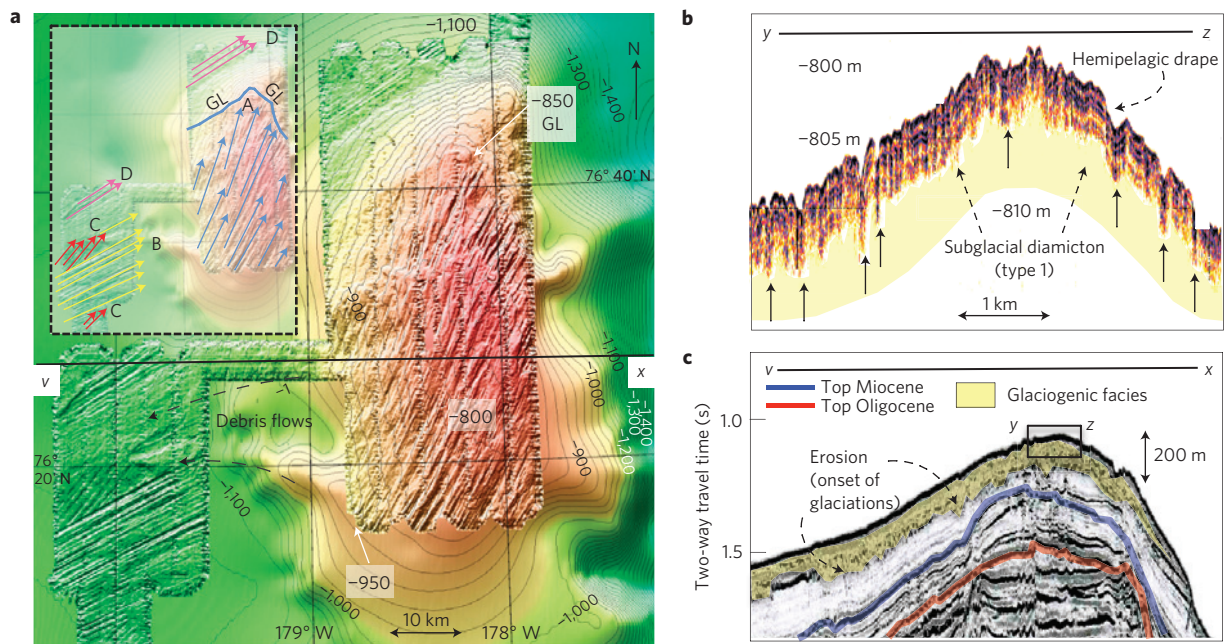


**Figure 2 | Evidence of grounded ice and glacial sedimentation on the Arlis Plateau (Fig. 1).** **a**, Bathymetric map with sets of different streamlined glacial lineations (SGL) overprinting each other. Note that SGL on the Arlis Plateau cease at a depth of 850 m in the north (interpreted as grounding line; GL) and continue to a depth of more than 950 m towards south-southwest. Top left inset: interpretation of flow direction of grounded ice sheets, their relative age (A–D, youngest to oldest) and GL of set A. **b**, Parasound image from top of Arlis Plateau (location marked in **c**) indicating a drape of hemipelagic sediments on streamlined subglacial diamicton. Arrows indicate streamlined subglacial grooves draped by overlying sediments. **c**, Data from seismic line 20080065 (v–x, location marked in **a**) with well-stratified hemipelagic sediments overlain by acoustically diffuse facies of glacial origin. Reflector stratigraphy is from ref. 21.

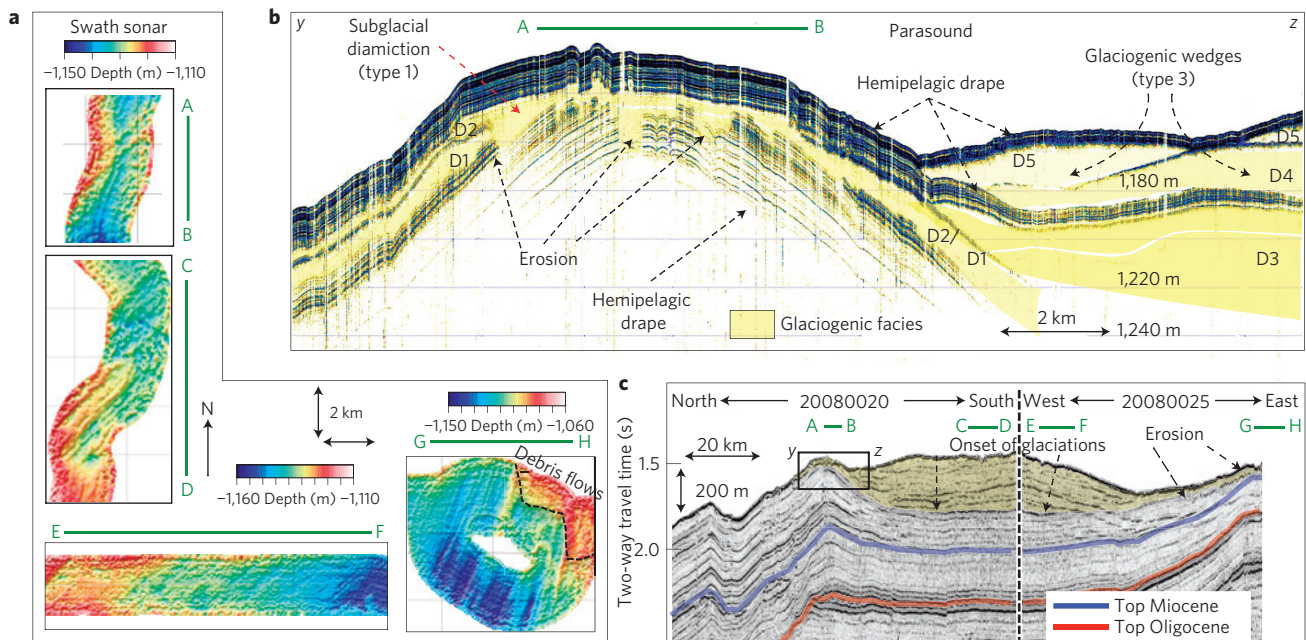


**Figure 3 | Glaciogenic fans and SGL on the East Siberian continental slope.** **a**, Seafloor morphology along the track lines. Location of sections A–B to G–H are marked in **b, c**. **b**, Parasound image (y–z, for location see **c**) exhibits well-stratified hemipelagic mud intercalated with transparent layers and wedges (diamicton D1 to D5). For the oldest glacial events (D1, D2), the location of the former grounding line is interpreted in a depth range from 1,140 to at least 1,180 m present water depth, where erosion and lineations are observed (**a**, A–B). **c**, Seismic lines 20080020 and 20080025 exhibit well-stratified and undisturbed Neogene strata, overlain by glaciogenic fan deposits and separated by an erosional discontinuity (interpreted as onset of glaciations). Reflector stratigraphy is from ref. 21.

continental slope (Fig. 4a,b). Therefore, deeper areas adjacent to the Arlis Plateau must have underlain this ice shelf, which we propose was also the cause of the glacial erosion on the Mendeleev Ridge<sup>17</sup>,

110 km farther north. Thus, thicker ice sheets previously formed along the ESCM would have had a large potential for the formation of ice shelves and large icebergs in the Arctic Ocean.

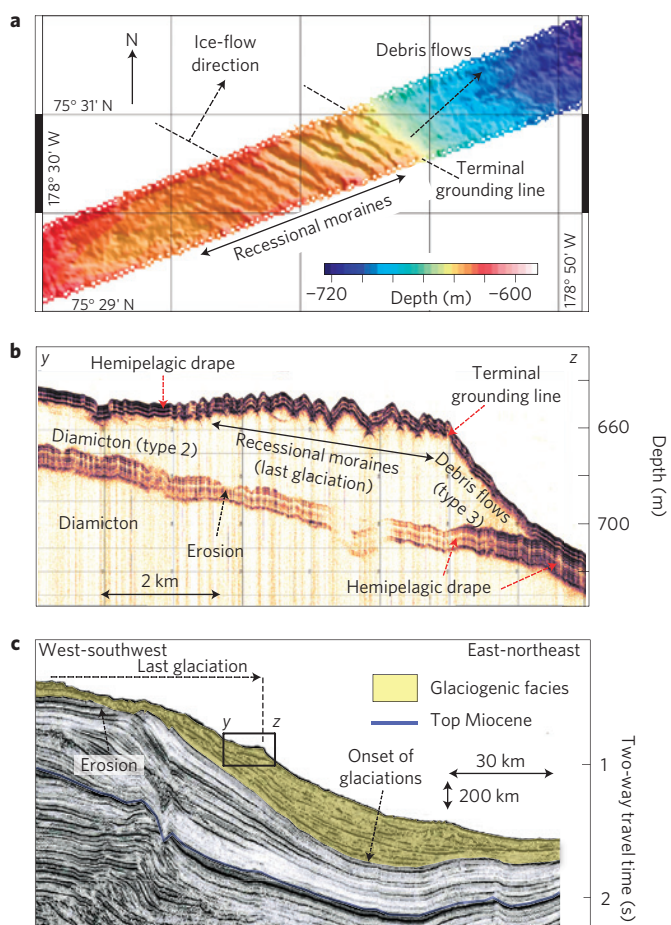


**Figure 4 | Glaciogenic facies and moraines on the East Siberian continental slope.** **a**, Swath sonar image along Parasound profile **(b)** exhibit small-scale ridges transverse to the ice-flow direction **a**. **b**, Parasound profile with two units of diamicton overlain by hemipelagic sediments (for location see **c**). **c**, Seismic line 20080040 with well-stratified progradational sediments of mostly Neogene age<sup>21</sup> overlain by facies of glacial origin (highlighted in yellow).

Obtaining a chronological framework for ice-proximal deposits and grounding events from longer cores remains a major challenge, because the acoustically transparent diamicton units described here have not yet been dated. All layers and wedges of massive diamicton are draped by, or intercalate with, hemipelagic mud that postdates the last grounding event or previous glaciations, respectively (Figs 2b, 3b, 4b). Mud thickness ranges from 3 m on top of the Arlis Plateau (Fig. 2b) to 20 m on the ESCM, where the earliest grounding events are draped conformably (Fig. 3b). For the past 120 kyr, mean hemipelagic sedimentation rates are 0.05–0.062 m kyr<sup>-1</sup> in the area between the Chukchi Borderland and the ESCM (refs 17,28). Thus, initial grounding associated with the onset of glacial deposition would probably have occurred during the middle Pleistocene or earlier. We suggest that this change marks the onset of Quaternary glaciations on the Pacific side of the Arctic Ocean (Figs 3c, 4c). Grounding and erosion of older strata in deep water suggest that this initial glaciation was more intense than younger glaciations. The initial glaciation on the ESCM is followed by at least five subsequent glaciations as indicated by the number of glaciogenic wedges that intercalate with well-stratified hemipelagic sediments (Fig. 3b). The advance of an ice sheet to 650 m.b.p.s.l. on the ESCM (Fig. 4a,b) is the youngest that we have identified. It is thought that this event occurred before the LGM because the sedimentation rates<sup>17,28</sup> do not allow the

accumulation of 5 m of hemipelagic mud on top of the moraines in post-LGM times.

As described here for the first time, the ESCM has proved to be a key location for a better understanding of the glacial history of the western Arctic. The apparent lack of a large ice sheet during times of the LGM implies significantly different climatic boundary conditions compared with earlier Arctic glaciations with implications for atmospheric circulation, in particular sources and distribution of moisture<sup>2,13</sup>. For the formation and stability of thick ice shelves in the Arctic Ocean the influx of warmer Atlantic water to the Arctic must have been reduced<sup>11</sup>. Owing to enhanced albedo and decreased ocean–atmosphere heat exchange, these ice masses contributed to the stability of glacial arctic climates. At glacial terminations, ice masses on the ESCM would have provided additional sources of fresh water to the Arctic Ocean, influencing the meridional overturning circulation in the North Atlantic and thus global climate<sup>15,29</sup>. With our evidence of a glaciated continental margin of East Siberia the idea of thick marine Pleistocene ice sheets in the western Arctic Ocean<sup>25</sup> is revitalised.

## Methods

The results of bathymetric, sediment echosounding and seismic surveys were obtained during the German RV *Polarstern* cruise ARK-XXIII/3 in 2008 and the South Korean RV *Araon* cruise ARA03B in 2012.

**Bathymetry.** On RV *Polarstern* the bathymetric survey was carried out using the hull-mounted ATLAS HYDROGRAPHIC HYDROSWEPT DS2, a deep-sea multibeam swath sonar system operated in the hard-beam mode with a frequency of 15.5 kHz, a resolution of 59 single depth points per ping and an opening angle of 90°, which results in a swath width of twice the water depth with a vertical resolution of <1% of the water depth. The mean sound velocity of the water column was calculated from DS2 crossfan calibration and conductivity–temperature–depth sensor data. On RV *Araon* the swath bathymetry survey was conducted using hull-mounted KONGSBERG EM122 multibeam echosounder operated with a frequency of 12 kHz, a resolution of 432 depth points per ping and an opening angle of 140°, which results in a swath width of six times the water depth with a vertical resolution of 0.2% of the water depth. Bathymetric data editing was carried out before export into ASCII-format (longitude, latitude, depth) suitable for plotting bathymetric charts using CARIS HIPS and SIPS and GMT software, respectively.

**Parasound sediment echosounding.** Sub-bottom profiling data were acquired on RV *Polarstern* using the parametric hull-mounted system ATLAS HYDROGRAPHIC PARASOUND DS III-P70. Primary operating frequencies were 18.75 and 22.95 kHz with a secondary sediment-penetrating frequency of 4.2 kHz, a beam angle of 4° and a pulse length of 2. The vertical resolution was about 0.2 m. Data visualization and processing was carried out using ATLAS PARASTORE-3 software. The vertical scale on profiles has been converted from travel time to metres using a constant sound velocity of 1.5 km s<sup>-1</sup>, which explains minor differences in water depth between Parasound and swath sonar data.

**Reflection seismic.** For the multichannel seismic (MCS) data acquisition on RV *Polarstern* a 3,000-m-long streamer (240 active channels, group interval of 12.5 m) and an air gun array of four G-Guns (total volume of 32 l, fired with 200 bar every 15 s) were used. After acquisition, the MCS data were demultiplexed and common-depth-point sorted (25 m CDP interval). Using a band pass filter of 10–100 Hz the data were filtered and a velocity model was determined for each seismic line. Afterwards, the spherical divergence and the normal moveout were corrected. The multiples were attenuated by f–k filtering. Finally, the seismic data were stacked and migrated in the omega–x domain. The vertical resolution of the AWI MCS data is about 15 m below the sea floor (using a seismic velocity of 1.8 km s<sup>-1</sup> and a peak frequency of 35 Hz). The horizontal resolution of the AWI MCS data is about 40 m in a depth of 50 m below the sea floor (using a seismic velocity of 1.8 km s<sup>-1</sup> and a peak frequency of 35 Hz). The vertical scale in metres (Fig. 2d) refers to sediment thickness above top Miocene calculated from velocity data of ref. 21 (1.9 km s<sup>-1</sup>). Tertiary marker horizons (top Miocene, top Oligocene; Figs 2d, 3c–4c) are based on a correlation of regional seismic lines with well data<sup>21</sup>.

Received 25 February 2013; accepted 2 July 2013; published online 11 August 2013

## References

- Ehlers, J. & Gibbard, P. L. The extent and chronology of Cenozoic global glaciation. *Quat. Internat.* **164–165**, 6–20 (2007).

2. Svendsen, J. I. *et al.* Late Quaternary ice sheet history of Northern Eurasia. *Quat. Sci. Rev.* **23**, 1229–1272 (2004).
3. England, J. H., Furze, M. F. A. & Doupé, J. P. Revision of the NW Laurentide Ice Sheet: implications for paleoclimate, the northeast extremity of Beringia, and Arctic Ocean sedimentation. *Quat. Sci. Rev.* **28**, 1573–1596 (2009).
4. Batchelor, C. L., Dowdeswell, J. A. & Pietras, J. T. Variable history of Quaternary ice-sheet advance across the Beaufort Sea margin, Arctic Ocean. *Geology* **41**, 131–134 (2013).
5. Alekseev, M. N. Paleogeography and geochronology in the Russian Eastern Arctic during the second half of the Quaternary. *Quat. Intern.* **41/42**, 11–15 (1997).
6. Gualtieri, L., Vartanyan, S. L., Brigham-Grette, J. & Anderson, P. M. Evidence for an ice-free Wrangel Island, northeast Siberia during the Last Glacial Maximum. *Boreas* **34**, 264–273 (2005).
7. Brigham-Grette, J. & Gualtieri, L. Letter to the Editor. *Quat. Sci. Rev.* **62**, 227–232 (2004).
8. Polyak, L., Edwards, M. H., Coakley, B. J. & Jakobsson, M. Ice shelves in the Pleistocene Arctic Ocean inferred from glaciogenic deep-sea bedforms. *Nature* **410**, 453–459 (2001).
9. Polyak, L. V., Darby, D. A., Bischoff, J. F. & Jakobsson, M. Stratigraphic constraints on late Pleistocene glacial erosion and deglaciation of the Chukchi margin, Arctic Ocean. *Quat. Res.* **67**, 234–245 (2007).
10. Jakobsson, M. *et al.* Glacial geomorphology of the Central Arctic Ocean: The Chukchi Borderland and the Lomonosov Ridge. *Earth Surf. Proc. Landf.* **33**, 526–545 (2008).
11. Jakobsson, M. *et al.* An Arctic Ocean ice shelf during MIS 6 constrained by new geophysical and geological data. *Quat. Sci. Rev.* **29**, 3505–3517 (2010).
12. Kristoffersen, Y. *et al.* Seabed erosion on the Lomonosov Ridge, central Arctic Ocean: A tale of deep draft icebergs in the Eurasia Basin and the influence of Atlantic water inflow on iceberg motion? *Paleoceanography* **19**, PA3006 (2004).
13. Stauch, G. & Gualtieri, L. Late Quaternary glaciations in northeastern Russia. *J. Quat. Sci.* **23**, 545–558 (2008).
14. Glushkova, O. Yu. Late Pleistocene Glaciations in North-East Asia. *Dev. Quat. Sci.* **15**, 865–875 (2011).
15. Hu, A. *et al.* Influence of Bering Strait flow and North Atlantic circulation on glacial sea-level changes. *Nature Geosci.* **3**, 118–121 (2010).
16. Rohling, E. J. *et al.* Antarctic temperature and global sea level closely coupled over the past five glacial cycles. *Nature Geosci.* **557**, 500–504 (2009).
17. Stein, R. *et al.* Towards a better (litho-) stratigraphy and reconstruction of quaternary paleoenvironment in the Amerasian Basin (Arctic Ocean). *Polarforschung* **79**, 97–121 (2010).
18. Dowdeswell, J. A., Ottesen, D., Rise, L. & Craig, J. Identification and preservation of landforms diagnostic of past ice-sheet activity on continental shelves from three-dimensional seismic evidence. *Geology* **35**, 359–362 (2007).
19. Davies, T. A. *et al.* (eds) *Glaciated Continental Margins. An Atlas of Acoustic Images* (Chapman/Hall, 1997).
20. Dowdeswell, J. A. *et al.* Submarine glacial landforms and rates of ice-stream collapse. *Geology* **36**, 819–822 (2008).
21. Hegewald, A. & Jokat, W. Relative sea level variations in the Chukchi region - Arctic Ocean - since the late Eocene. *Geophys. Res. Lett.* **40**, 803–807 (2013).
22. Tulaczyk, S., Kamp, W. B. & Engelhardt, H. F. Basal mechanics of Ice Stream B, West Antarctica. 1. Till mechanics. *J. Geophys. Res.* **105**, 463–481 (2000).
23. Lindén, M. & Möller, P. Marginal formation of De Geer moraines and their implications to the dynamics of grounding-line recession. *J. Quat. Sci.* **20**, 113–133 (2005).
24. O'Regan, M. *et al.* Constraints on the Pleistocene chronology of sediments from the Lomonosov Ridge. *Paleoceanography* **23**, PA1S19 (2008).
25. Grosswald, M. G. & Hughes, T. J. The Russian component of an Arctic Ice Sheet during the Last Glacial Maximum. *Quat. Sci. Rev.* **21**, 121–146 (2002).
26. Greve, R., Wyrwoll, K.-H. & Eisenhauer, A. Deglaciation of the Northern Hemisphere at the onset of the Eemian and Holocene. *Ann. Glaciol.* **28**, 1–8 (1999).
27. Basilian, A. C., Nikol'skiy, P. A. & Anisimov, M. A. Pleistocene glaciation of the New Siberian Islands - no more doubt. *IPY News* **12**, 7–9 (2008) AARI.
28. Polyak, L. & Jakobsson, M. Quaternary sedimentation in the Arctic Ocean: Recent advances and further challenges. *Oceanography* **24**, 52–64 (2011).
29. Peltier, W. R. Rapid climate change and Arctic Ocean freshening. *Geology* **35**, 1147–1148 (2007).

### Acknowledgements

We are grateful for the support of the captains and crews of the RV *Polarstern* and RV *Araon* during the cruises ARK-XXIII/3 and ARA03B, respectively. We thank S. Hanisch, O. Thomas and J. Collins for improvement of text and figures. This publication is a contribution to the research programme PACES, topic 3 (Lessons from the Past) of the Alfred Wegener Institute, Helmholtz Centre for Polar und Marine Research (AWI) and the projects K-PORT (PM11080) and K-Polar (PP13030) of the Korea Polar Research Institute (KOPRI). This research was financially supported by AWI, KOPRI and MOF of Korea.

### Author contributions

F.N. participated in both expeditions in 2008 and 2012, interpreted the hydro-acoustic data and wrote the first draft of the manuscript. J.K.H. led the bathymetric survey on RV *Araon*, A.H. processed and plotted the seismic multichannel data. H.K. acquired and processed multibeam data on RV *Araon*, S.K. compiled bathymetric data of KOPRI and conducted image processing. L.J. acquired and processed multibeam data on RV *Polarstern* and carried out image processing. J.M. contributed to Parasound data acquisition on RV *Polarstern*, R.S. and W.J. led the geological and geophysical data acquisition, respectively, on RV *Polarstern* and S-I.N. led the geological data acquisition on RV *Araon*. All authors contributed to writing the paper and analysing the results. S-H.K. led the K-PORT project and contributed to the geophysical survey on RV *Araon*.

### Additional information

Data are available at <http://dx.doi.org/10.1594/PANGAEA.810972>. Reprints and permissions information is available online at [www.nature.com/reprints](http://www.nature.com/reprints). Correspondence and requests for materials should be addressed to F.N. or J.K.H.

### Competing financial interests

The authors declare no competing financial interests.